Journal of Constructional Steel Research 148 (2018) 409–421

Contents lists available at ScienceDirect

Journal of Constructional Steel Research

Probabilistic residual drift assessment of SMRFs with linear and nonlinear viscous dampers

A. Yahyazadeh, M. Yakhchalian *

Department of Civil Engineering, Faculty of Engineering and Technology, Imam Khomeini International University, PO Box 34149-16818, Qazvin, Iran

ARTICLE INFO

Article history:
Received 2 December 2017
Received in revised form 11 May 2018
Accepted 27 May 2018
Available online xxxx

Keywords:
Fluid viscous damper
Maximum residual interstory drift ratio
Incremental dynamic analysis
Residual drift fragility
Vertical distribution of damping coefficients

ABSTRACT

Maximum Residual Interstory Drift Ratio (MRIDR) is one of the most important Engineering Demand Parameters (EDPs) for evaluating the safety of structures after the occurrence of an earthquake. This EDP is used as an index to decide about the retrofit or demolition of structures. The main purpose of this study is to evaluate the effects of using linear and nonlinear Fluid Viscous Dampers (FVDs) on the MRIDR response of steel Special Moment Resisting Frames (SMRFs) with FVDs. Moreover, two vertical distributions of damping coefficients including Uniform Distribution (UD) and Interstory Drift Proportional Distribution determined based on the first mode deformations (IDPD) are compared for the structures considered. The values of median MRIDR capacity, median Sa_{RD}, corresponding to different MRIDR levels are determined by performing Incremental Dynamic analyses (IDAs). After computing the median Sa_{RD} for a specified MRIDR level and its corresponding logarithmic standard deviation, the Mean Annual Frequency (MAF) of exceeding that MRIDR level (λ_{RD}) is computed. Based on the results, the values of median Sa_{RD} for structures with linear FVDs are higher than those for structures with nonlinear FVDs, and hence the values of λ_{RD} corresponding to structures with linear FVDs are lower than those for structures with nonlinear FVDs. In addition, for structures with a soft story, using IDPD to determine damping coefficients results in higher median Sa_{RD} values, and hence lower λ_{RD} values.

1. Introduction

Maximum Interstory Drift Ratio (MIDR) has been extensively used as an Engineering Demand Parameter (EDP) in most of the previous studies existing in the technical literature. MIDR is the maximum of all peak Interstory Drift Ratios (IDRs) observed along the height of a multi-story frame, where peak IDR for a particular story is the peak of the absolute values of IDR in the IDR time history response of the story. MIDR is a useful parameter to predict structural damage or collapse. Although collapse prediction is an important issue during life of structures, another question is that if structures can be used after strong ground motion or not. Recently, some researchers have focused on investigating Maximum Residual Interstory Drift Ratio (MRIDR) response of structures. Residual Interstory Drift Ratio (RIDR) for a particular story is the last (absolute) value of the IDR time history of the story. The MRIDR is the maximum RIDR of all the stories of the frame. Ruiz-García and Miranda [1] reported that the amplitude and height-wise distribution of residual drift demands strongly depend on building frame mechanism, hysteretic behavior of components, the height-wise system structural overstrength and ground motion intensity. Bojórquez and Ruiz-García [2] concluded that steel structures designed for MIDR demand subjected to narrow-band ground motion records may experience large permanent displacements that may lead to take the decision of demolishing them. Christopoulos et al. [3] reported that residual drift response strongly depends on post-yielding stiffness, maximum ductility demand and unloading stiffness of system. Ruiz-García and Aguilar [4] presented a procedure to evaluate the aftershock seismic performance of structures, which considers residual drift demands after the mainshock. The results of their study indicated that the collapse potential under aftershocks depends on the modeling approach. Moreover, it was concluded that the aftershock capacity corresponding to demolition (i.e., the aftershock capacity corresponding to reaching a residual interstory drift value that necessitates the demolition of structure) is lower than that of the aftershock collapse capacity, which means that this parameter is a better measure of the structure residual capacity against aftershocks. Sultana and Youssef [5] investigated the seismic performance of steel Moment Resisting Frames (MRFs) utilizing superelastic Shape Memory Alloys (SMAs). In their study, maximum and residual interstory drifts were used to assess the seismic performance of the structures considered. They showed that the optimum use of superelastic SMA in the beam to column connections could minimize the residual drifts of the structures. McCormick et al. [6] conducted a study to evaluate the psychological and physiological effects of residual drifts on occupants of buildings in Japan. They reported that residual interstory drifts of about 0.5% are perceptible for occupants

* Corresponding author.
E-mail address: yakhchalian@eng.ikiu.ac.ir (M. Yakhchalian).

https://doi.org/10.1016/j.jcsr.2018.05.031
0143-974X/

of building, and reaching a residual interstory drift of 1.0% causes the dizziness of occupants. Thus, they suggested the residual interstory drift of 0.5% as the permissible residual drift level. FEMA P-58 [7] presents a simplified equation to estimate residual drift, and a building repair fragility based on residual drift. Moreover, Appendix C in this document includes a table identifying four levels of residual interstory drift corresponding to four damage states (DS1-DS4). The first level (DS1) is defined as reaching a residual interstory drift of 0.2%, which represents a state that no structural readjustment is required; however, building requires repairs to nonstructural components. The second level (DS2) occurs when residual interstory drift approaches to 0.5%, implying that both structural and nonstructural components require realignment and repair. The third level (DS3) corresponds to a residual interstory drift of 1.0% in which significant structural readjustment is required to maintain the safety of building; however, the repair costs of the building are not economically feasible. Finally, the fourth level (DS4) is known as reaching a residual interstory drift of 1.0% to 4.0% as a function of building ductility, that is, building is in danger of collapse due to aftershocks. These residual interstory drift levels are approximate, and have been determined according to a combination of judgment and limits proposed in FEMA 356 [8]. Kitayama and Constantinou [9] applied four residual interstory drift levels of 0.2%, 0.5%, 1.0% and 2.0%, corresponding to the four aforementioned damage states, for probabilistic assessment of residual drift performance of structures with fluidic self-centering systems.

In recent decades, using supplemental damping systems has been developed to achieve higher performance levels in the design of new structures and improve the seismic performance of existing structures [10]. Among supplemental damping systems, Fluid Viscous Dampers (FVDs), which include linear and nonlinear FVDs, are more widely used [11]. The force generated in a FVD is determined as follows:

$$F = C|\dot{u}|^{\alpha}\, sgn(\dot{u}) \tag{1}$$

where C is the damping coefficient, $\dot{u}$ is the relative velocity between two ends of damper and α is the velocity exponent of damper. A damper with $\alpha = 1.0$ is called linear FVD and a damper with $\alpha \neq 1.0$ is called nonlinear FVD. Christopoulos and Filiatrault pointed out that the value of α is in the range of 0.2–1.0 for seismic applications [12]. FVDs manufactured by Taylor Devices Company [13] have velocity exponents that are in the range of 0.3–1.0, whereas those manufactured by Jarret Structures Company [14] have velocity exponents in the range of 0.1–0.4. Simplicity in design is one of the important advantages of FVDs, which makes them more popular than other dampers [15]. Several studies have been performed on the seismic performance of structures with FVDs. Mansoori and Moghadam [16] investigated using different distributions of FVDs to reduce seismic responses of asymmetric structures. They concluded that the distribution of FVDs has a considerable effect on the modal damping ratios of structures. Kim et al. [17] evaluated the seismic performance of special truss moment frames equipped with FVDs. They showed that adding FVDs to special truss moment frames has the most significant effect on the seismic fragility in the complete damage state. Jamshidiha et al. [18] proposed three advanced scalar Intensity Measures (IMs) to reliably predict the collapse capacity of steel Special Moment Resisting Frames (SMRFs) equipped with FVDs. These IMs include information about the spectral shape and duration of ground motion records. Karavasilis and Seo [19] evaluated the seismic structural and non-structural performance of self-centering and conventional Single-Degree-of-Freedom (SDOF) systems with FVDs. They showed that decreasing the strength of SDOF systems decreases total accelerations, whereas added damping increases total accelerations and decreases residual displacements. However, in some cases, added damping may increase residual displacements of bilinear elastoplastic SDOF systems. Bahnasy and Lavan [20] reported that by decreasing α, MRIDR responses of structures with FVDs increase, whereas damper forces decrease. Different procedures exist in the technical literature, to determine the viscous damping coefficients for a structure equipped with FVDs. Whittaker et al. [21] presented a procedure, which is based on the equivalent lateral force and response spectrum analysis methods of the 2000 NEHRP Provisions [22], for seismic design of buildings with energy dissipation systems. This procedure is the main reference of Chapter 18 in ASCE 7 [23] that is related to the design of new buildings with energy dissipation systems, including buildings equipped with FVDs. Landi et al. [24] proposed a procedure for the direct determination of the supplemental viscous damping required for the seismic retrofit of structures with FVDs. The advantage of this procedure is that it does not require performing several iterations. It is noteworthy that there are several vertical distributions of damping coefficients in the technical literature. Some of these distributions are Uniform Distribution (UD), Mass Proportional Distribution (MPD), Story Stiffness Proportional Distribution (SSTPD), Story Shear Proportional Distribution (SSPD) and Interstory Drift Proportional Distribution determined based on the first mode deformations (IDPD) [25].

Nowadays, the seismic assessment of existing structures and design of new structures is often performed by employing probabilistic approaches, such as that outlined by the Performance-Based Earthquake Engineering (PBEE) framework [26–29], developed by researchers in Pacific Earthquake Engineering Research (PEER) center. The PEER PBEE framework has four stages including seismic hazard analysis, seismic demand analysis, damage analysis and loss analysis. The result of each stage is expressed by an intermediate variable. These intermediate variables are IM, EDP, Damage Measure (DM) and Decision Variable (DV), respectively. One of the important issues in using the PEER PBEE framework is to select the proper EDP. EDPs are important parameters to evaluate the seismic performance of structures, and include structural responses such as force, maximum floor acceleration, MIDR, MRIDR, etc. By applying the two first stages of the PEER PBEE framework, the Mean Annual Frequency (MAF) of exceeding a specified level of an EDP can be obtained. Dall'Asta et al. [30] showed that MAFs of exceeding low levels of MIDR (e.g., MIDR < 0.01) for structures with nonlinear FVDs are lower than those for structures with linear FVDs, whereas for higher levels of MIDR, the trend is reversed. Tubaldi et al. [31] evaluated the effects of nonlinear behavior of FVDs on seismic response of SDOF systems in a probabilistic framework. They concluded that using deterministic approaches that neglect the dispersion of response has some limitations for the assessment of system reliability. Dall'Asta et al. [32] investigated the effect of variability in FVD properties due manufacturing on the probabilistic performance of SDOF systems equipped with linear and nonlinear FVDs. They concluded that short-period SDOF systems are more sensitive to FVD property variation than long-period ones. In the last decade, MRIDR is one of the important EDPs that has attracted the attention of researchers. Ruiz-García and Miranda [33] implemented a probabilistic approach to estimate MRIDR demands in buildings, and used this approach to compute residual drift demand hazard curves for multi-story frames. Kitayama and Constantinou [9] reported that the important parameter affecting the residual drift fragilities of structures with fluidic self-centering systems is the increase in the ultimate capacity of self-centering device-brace system. Daylami and Mahdavipour [34] performed a probabilistic assessment of MRIDR response of dual systems including Buckling Restrained Braced Frames (BRBFs). By comparing the obtained residual drift demand hazard curves, they concluded that using BRBFs as a dual system significantly improves the residual drift performance, when compared with using BRBFs alone. Although there are some studies, in the technical literature, that have evaluated MAFs of exceeding different MRIDR levels, but research works on probabilistic assessment of MRIDRs for structures with FVDs are rare. Dimopoulos et al. [35] investigated the potential of post-tensioned Self-Centering Moment Resisting Frames (SC-MRFs) and FVDs to mitigate the economic seismic losses in steel buildings. They considered both the probability of collapse and the probability of demolition due to excessive RIDRs, using the PEER PBEE methodology, and concluded that supplemental viscous damping is

more effective than post-tensioning in reducing the repair cost for seismic intensities equal to or lower than the Maximum Considered Earthquake (MCE). Tzimas et al. [36] studied the collapse risk and residual drift performance of steel buildings using SC-MRFs and FVDs in near-fault regions. They found that the SC-MRF with FVDs achieves significant reductions in collapse risk and probability of exceedance of MRIDR values compared with a MRF.

The purpose of this study was to assess the effects of using linear and nonlinear FVDs and the distributions of their respective damping coefficients on the MRIDR response of SMRFs equipped with FVDs, in a probabilistic framework. For this purpose, three steel SMRFs were selected and their performance was improved by adding FVDs. Two vertical distributions of damping coefficients, i.e., UD and IDPD, were considered to equip each of the steel SMRFs with FVDs. Then, by performing Incremental Dynamic Analyses (IDAs) [37], the median MRIDR capacities (median Sa_{RD}) of the SMRFs equipped with linear and nonlinear FVDs were computed, and their corresponding fragility curves were developed. By combining the fragility curves, corresponding to different MRIDR levels, for each of the structures and the seismic hazard curve for the pseudo spectral acceleration at the fundamental period of the structure, MAFs of exceeding different levels of MRIDR (i.e., λ_{RD} values) were calculated. Finally, conclusions were drawn on the effects of damper nonlinearity and vertical distributions of damping coefficients on the residual drift performance of SMRFs with FVDs.

2. Structures selected and modeling

In this study, 3- and 9-story steel SMRF structures with a regular plan and perimeter frame system were considered. These structures were designed for seismic conditions in Los Angeles, seismic zone 4 defined in UBC 94 [38], according to the post-Northridge seismic design criteria and are part of the SAC steel project [39]. More details about these structures are available in FEMA-355C [40]. In addition, to assess the effect of soft story, a new structure (i.e., 3-story-h_1-1.4 structure) was generated by increasing the first story height of the 3-story structure by a factor of 1.4. Thus, the first story in the new structure is a soft story that has increased ductility demands. This soft-story structure is representative of a structure that requires seismic retrofit. Other researchers (e.g., Apostolakis and Dargush [41] and Hamidia et al. [42]) have also applied such a method to generate soft-story structures. It was assumed that the structures were located at a site with soil class D in Los Angeles having latitude 33.996°N and longitude 118.162°W, which is a typical non-near-field site with high seismicity [43]. The parameters of the ASCE 7 [23] risk-targeted Maximum Considered Earthquake (MCE_R) response spectrum for the site of interest, which are $S_{MS} = 2.167$ g and $S_{M1} = 1.124$ g, were obtained from the USGS website [44]. Then, the seismic performance of the structures was improved by adding FVDs. Diagonal and horizontal configurations are commonly used for installing FVDs to stories of buildings. In the first configuration, displacement of damper is less than interstory drift, whereas in the second one, displacement of damper is equal to interstory drift. Thus, the second configuration is more effective than the first one. However, in this study, similar to many studies existing in the technical literature (e.g., [30, 42, 45]), the diagonal configuration was selected to equip the considered structures with FVDs. Fig. 1 indicates the structures considered and the arrangement of FVDs in these structures.

To investigate the effects of damper nonlinearity, four values of velocity exponent, i.e., $\alpha = 0.25$, 0.5, 0.75 and 1.0 were considered for the FVDs. The Open System for earthquake engineering simulation (OpenSees) [46] was used to model the structures. In order to consider the nonlinear behavior of columns, distributed plasticity force-based beam-column elements were applied. Each of the force-based beam-column elements has five integration points along its length, and a fiber section assigned to these integration points. The nonlinear behavior of each fiber was simulated using the Menegotto-Pinto steel model (i.e., the Steel02 material in the OpenSees), assuming an elastic modulus of 200 GPa and a strain hardening ratio of 0.002. Therefore, cyclic deterioration in columns was neglected. It should be mentioned that a strain hardening ratio of 0.002 has been used in other studies such as those performed by Seo et al. [47] and Kitayama and Constantinou [9]. Using a concentrated plasticity approach [43, 48], beams were modeled by elastic beam-column elements and two nonlinear zero-length rotational spring elements at their ends, representing flexural plastic hinges. The modified Ibarra-Krawinkler model (Bilin) [49] was applied to simulate the behavior of the zero-length elements. The second order P–Δ effects of gravity columns were considered by a leaning column located beside the frame, connected to the frame with axially rigid truss elements. The leaning column consists of elastic beam-column elements having areas 100 times those for the frame columns. Zero-length rotational spring elements with very small stiffness values were used to connect these beam-column elements to the nodes located in the floor levels, which are at the ends of the aforementioned axially rigid truss elements. Table 1 presents the first to third mode periods of the structures considered.

3. Equipping the structures with supplemental FVDs

In this study, the procedure proposed by Landi et al. [24] was used to determine the supplemental viscous damping required to enhance the seismic performance of the structures. For this purpose, the values of yield base shear (V_y) and roof displacement corresponding to the desired performance level of the structures should be obtained. To obtain V_y, base shear-roof displacement curves of the structures were determined by using nonlinear static pushover analyses, considering lateral load distributions proportional to the first mode shapes of the structures. Each of these curves was plotted up to the roof displacement

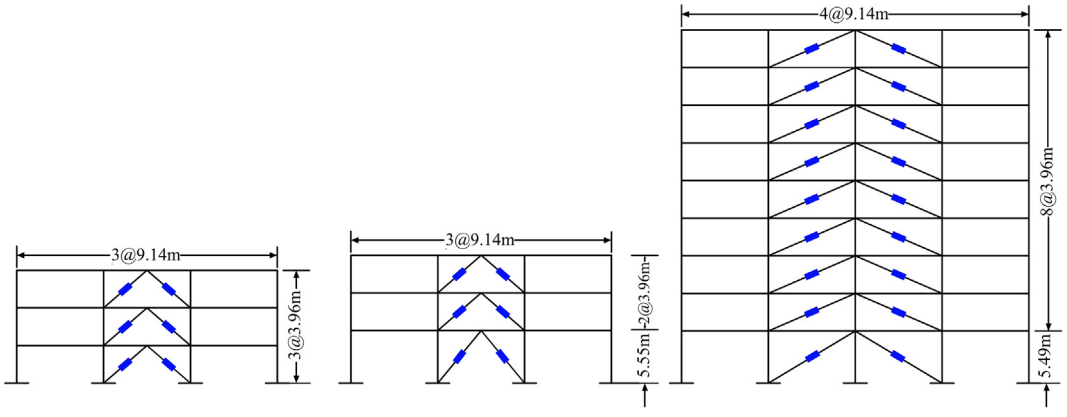

Fig. 1. Structures considered and the arrangement of FVDs in these structures.

Table 1
First to third mode periods of the structures considered (*s*).

Structure	First mode	Second mode	Third mode
3-story	0.95	0.30	0.14
3-story-h_1-1.4	1.20	0.36	0.15
9-story	2.08	0.78	0.44

corresponding to 85% of the maximum base shear. Then, V_y was calculated by converting the base shear-roof displacement curve to an idealized elasto-perfectly plastic curve, according to the method presented in the Italian building code [50]. A MIDR of 0.015 under the Design Basis Earthquake (DBE) of ASCE 7 [23] was selected as the target performance level to equip the structures with FVDs. In other words, the roof displacement corresponding to a MIDR of 0.015 is the target roof displacement. The DBE has a design response spectrum that is 2/3 times the MCE_R response spectrum, which usually has < 15% difference with the MCE response spectrum having 2.0% probability of exceedance in 50 years [51]. Fig. 2 shows the base shear-roof displacement curve and its corresponding idealized elasto-perfectly plastic curve for the 3-story structure.

The procedure applied to determine supplemental viscous damping ratios is based on using spectral capacity and demand curves in Acceleration Displacement Response Spectrum (ADRS) format. In general, the effective damping ratio for a structure equipped with FVDs is calculated as follows:

$$\xi_{eff} = \xi_i + \xi_h + \xi_v \tag{2}$$

where ξ_i is the inherent viscous damping ratio, ξ_h is the equivalent viscous damping ratio due to hysteretic behavior of structure and ξ_v is the supplemental viscous damping ratio. To compute ξ_{eff}, demand and capacity curves should be converted to the ADRS format. The idealized base shear-roof displacement (capacity) curve can be converted to the capacity spectrum as follows:

$$Sa = \frac{V_b}{M_1} \tag{3}$$

$$Sd = \frac{D_{roof}}{\Gamma_1 \varphi_{roof1}} \tag{4}$$

$$M_1 = \frac{\left(\sum_{i=1}^{N} m_i \varphi_{i1}\right)^2}{\sum_{i=1}^{N} m_i \varphi_{i1}^2} \tag{5}$$

$$\Gamma_1 = \frac{\sum_{i=1}^{N} m_i \varphi_{i1}}{\sum_{i=1}^{N} m_i \varphi_{i1}^2} \tag{6}$$

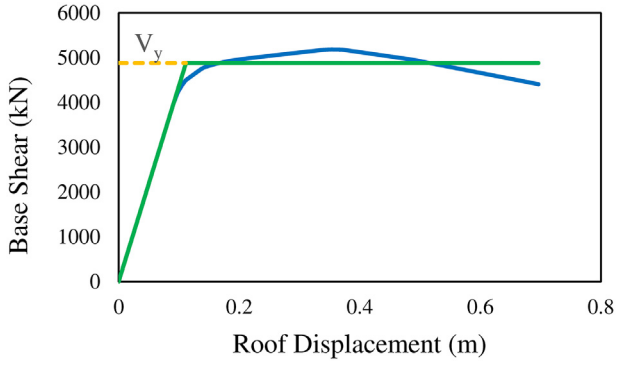

Fig. 2. Base shear-roof displacement curve and its corresponding idealized elasto-perfectly plastic curve for the 3-story structure.

where V_b is the base shear and M_1 is the effective modal mass of the first mode of structure; D_{roof} is the roof displacement and $\Gamma_1\varphi_{roof1}$ is the normalized modal participation factor [1, 33] that is calculated by multiplying the modal participation factor of the first mode of structure, Γ_1, by the modal deformation at the roof level corresponding to the first mode shape, φ_{roof1}. In Eqs. (5) and (6), φ_{i1} is the ordinate of the first mode shape at the top of the *i*th story, m_i is the mass of the *i*th story and *N* is the number of stories. Fig. 3 indicates the demand spectrum and the capacity spectrum of the 3-story structure, where Sd_m and Sa_y are the target roof displacement and the yielding acceleration in the ADRS format. In this figure, elastic acceleration demand (Sa_{el}) is the ordinate of the intersection point of the demand spectrum and the line drawn from the center of coordinates passing through the point corresponding to Sd_m on the capacity spectrum. The calculation of ξ_{eff} is dependent on parameter B, which is obtained from the following equation:

$$B = \frac{Sa_{el}}{Sa_y}. \tag{7}$$

After the calculation of B, ξ_{eff} can be obtained using a table presented by Ramirez et al. [45], which relates the values of B to their corresponding damping ratios.

Determining the supplemental viscous damping ratio, ξ_v, requires to consider the actual hysteretic behavior of structure using ξ_h, that is defined as:

$$\xi_h = \frac{2q_h}{\pi}\left(1 - \frac{1}{\mu}\right) \tag{8}$$

where μ is the ductility demand, and q_h is the ratio of the actual area of the hysteresis loop of structure to that of an idealized elasto-perfectly plastic system. Parameter q_h can be calculated according to the equation presented in ASCE 7 [23] as:

$$0.5 \le q_h = 0.67\frac{T_S}{T_1} \le 1.0 \tag{9}$$

where T_S is the transition period between the constant acceleration and constant velocity regions of ASCE 7 [23] design response spectrum, and T_1 is the fundamental period of structure. Assuming $\xi_i = 0.05$, parameter ξ_v can be calculated using the following equation:

$$\xi_v = \xi_{eff} - \left(\xi_i + \frac{2q_h}{\pi}\left(1 - \frac{1}{\mu}\right)\right). \tag{10}$$

When a structure equipped with FVDs experiences nonlinear deformations in its desired performance level, ξ_v can be obtained as follows:

$$\xi_v = \xi_{ve}.(\mu)^{1-\frac{\alpha}{2}} \tag{11}$$

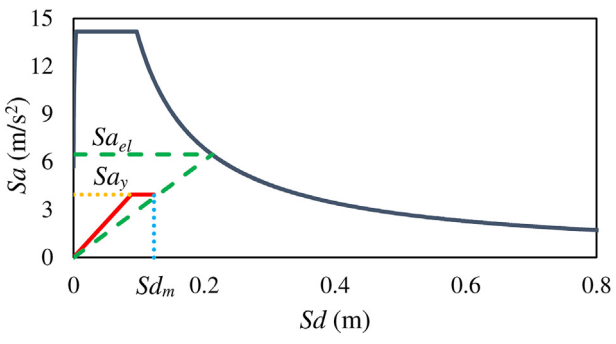

Fig. 3. Demand spectrum and the capacity spectrum of the 3-story structure.

where ξ_{ve} is the supplemental viscous damping ratio assuming a linear behavior for the structure. After attaching FVDs with a specific value of velocity exponent, α, to a structure, ξ_{ve} can be calculated as follows:

$$\xi_{ve} = \frac{\sum_{j=1}^{N_d} {f_j}^{1+\alpha} {\varphi_{rj1}}^{1+\alpha} {D_{roof}}^{\alpha-1} (2\pi)^{\alpha} T_1^{2-\alpha} \lambda_j C_j}{8\pi^3 \sum_{i=1}^{N_s} (m_i) {\varphi_{i1}}^2} \tag{12}$$

where N_d and N_s are the number of dampers and stories, respectively; D_{roof} is the roof displacement, C_j is the damping coefficient of the jth damper, $f_j = cos\ \theta_j$ is the displacement magnification factor, θ_j is the angle of damper direction with the horizontal axis, φ_{rj1} is the relative deformation between the horizontal degrees of freedom at the ends of the jth damper corresponding to the first mode shape, and φ_{i1} and m_i are the first mode shape ordinate at the top of the ith story and the mass of the ith story, respectively; and λ_j is a function of α, which can be determined from the relationship presented in [45]. In this study, two vertical distributions of damping coefficients including UD and IDPD were considered. UD was selected due to its simplicity, whereas the reason for the selection of IDPD is that using this distribution leads to higher damping coefficients for soft stories. By applying Eq. (12) and each of the distributions, the damping coefficients corresponding to these distributions can be obtained as [25]:

$$C = \frac{\xi_{ve} 8\pi^3 \sum_{i=1}^{N_s} (m_i) {\varphi_{i1}}^2}{\sum_{j=1}^{N_d} (2\pi)^{\alpha} T_1^{2-\alpha} \lambda_j {D_{roof}}^{\alpha-1} {f_j}^{1+\alpha} {\varphi_{rj1}}^{1+\alpha}} \tag{13}$$

$$C_k = \frac{\gamma_k \xi_{ve} 8\pi^3 \sum_{i=1}^{N_s} (m_i) {\varphi_{i1}}^2}{\sum_{j=1}^{N_d} (2\pi)^{\alpha} T_1^{2-\alpha} \lambda_j \gamma_j {D_{roof}}^{\alpha-1} {f_j}^{1+\alpha} {\varphi_{rj1}}^{1+\alpha}} \tag{14}$$

where C is the damping coefficient for all the dampers in the case of using UD, C_k is the damping coefficient of the dampers located at the kth story in the case of using IDPD, and γ_k is the interstory drift corresponding to the first mode shape of the structure in the kth story. The values of ξ_v, μ and D_{roof} for the considered structures are presented in Table 2. Given these values for each of the structures, Eqs. (11) to (14) were applied to determine the damping coefficients corresponding to UD and IDPD. Table 3 presents damping coefficients determined for one of the FVDs added to each of stories given different design scenarios for the structures. There are some studies in the technical literature that have investigated the effect of FVD supporting brace flexibility on the seismic response of structures with FVDs. Londoño et al. [52] proposed a filter design solution to size supporting braces of linear FVDs, and showed that using this procedure the behavior of brace-damper assembly within a specific frequency bandwidth is nearly as a pure dashpot. Lin and Chopra [53] pointed out that for a ratio of Maxwell relaxation time to the period of SDOF system < 0.02, brace flexibility has a small effect on the response of system. Thus, similar to the study performed by Hamidia et al. [42], to simulate FVDs, their supporting braces were considered as rigid. Furthermore, it was assumed that FVDs do not reach their stroke limits under seismic excitations. In other words, this assumption means that FVDs have been manufactured with strokes limits large enough to prevent reaching these limits under very large IDRs. Such an assumption has also been considered by other researchers [36, 47, 54, 55].

Using the results of pushover analyses, and assuming ξ_v equal to zero, Eqs. (2) to (9) were applied to determine the MIDR for each of the structures without FVDs under the DBE, in an iterative process. In each iteration of this process, a value for the roof displacement, D_{roof}, under the DBE was assumed, and after obtaining B and its corresponding ξ_h, the value of μ was calculated based on Eq. (8). Then, the value obtained from multiplying the yield displacement in the capacity spectrum by μ and $\Gamma_1 \varphi_{roof1}$ was compared with the assumed D_{roof}. If the value obtained for the roof displacement was close the assumed D_{roof} with an acceptable tolerance (i.e., with < 1% difference), the value of MIDR corresponding to D_{roof} was extracted from the results of pushover analysis. The values of MIDR under the DBE determined for the 3-story, 3-story-h_1-1.4 and 9-story structures without FVDs using the aforementioned process are 0.019, 0.023 and 0.021, respectively.

Table 2
Values of ξ_v, μ and D_{roof} for the considered structures.

Structure	ξ_v	μ	D_{roof} (cm)
3-story	0.138	1.466	4.130
3-story-h_1-1.4	0.238	1.106	6.343
9-story	0.139	1.362	14.882

4. Methodology used for probabilistic residual drift assessment of the structures

In this study, the IDA method [37] was applied as a tool for probabilistic residual drift assessment of the structures. For this purpose, $Sa(T_1)$ and MRIDR were respectively considered as IM and EDP for performing IDAs, assuming four levels of MRIDR (i.e., MRIDR = 0.2%, 0.5%, 1.0% and 2.0%) as limit states. In fact, for each of the structures, Sa_{RD} corresponding to a specified MRIDR level is a random variable that represents the distribution of $Sa(T_1)$ values resulting in that MRIDR level in the structure, obtained using different ground motion records. Given a ground motion record used for performing IDA, Sa_{RD} is the capacity of the structure to resist the specified MRIDR level, in terms of $Sa(T_1)$; and thus it is termed MRIDR capacity. To perform IDAs, 67 high-amplitude ground motion records used by Yakhchalian et al. [56–58], which were extracted from the general far-field ground motion set used by Haselton and Deierlein [43] including 78 ground motion records, were selected. Hamidia et al. [42] have also used a far-field ground motion set including 44 ground motion records, extracted from these 78 ground motion records, for seismic collapse assessment of the 3- and 9-story SAC buildings designed for Los Angeles, equipped with FVDs. It should be mentioned that to accurately compute MRIDR capacities, i.e., Sa_{RD} values, the analyses were continued with zero input acceleration at the end of each record until the structure came to rest. Moreover, if a MIDR of 0.15 was exceeded before reaching the desired value of MRIDR, analysis was stopped and $Sa(T_1)$ corresponding to MIDR = 0.15 was considered as MRIDR capacity, Sa_{RD}. The reason for this issue is that when MIDR is equal to 0.15, the building is considered as collapsed. A similar assumption has been used by Kitayama and Constantinou [9]. It should be mentioned that for obtaining Sa_{RD} values corresponding to a specified MRIDR level, the hunt and fill algorithm [37] was used to reduce the number of nonlinear dynamic analyses required. Fig. 4 illustrates the IDA curves of the 3-story structure equipped with FVDs assuming a uniform vertical distribution of damping coefficients (i.e., 3-story-UD structure) and α = 0.75, corresponding to MRIDR = 0.2% and 0.5%. Comparing Fig. 4(a) with Fig. 4(b) in the MRIDR range of 0–0.2% indicates that the global trends of the IDA curves in both the figures are similar, but differences between the IDA curves can be observed, which are due to using the hunt and fill algorithm.

Assuming a lognormal distribution for Sa_{RD} values, the probability of exceeding a specified value of MRIDR, x, given $Sa(T_1) = Sa$, can be calculated using the following equation:

$$P(RD|Sa) = P[RD \geq x \mid Sa(T_1) = Sa] = \Phi\left(\frac{\ln Sa - \ln \overline{Sa}_{RD}}{\sigma_{\ln Sa_{RD}}}\right) \tag{15}$$

where $\Phi()$ is the cumulative distribution function of the standard normal distribution; and $\ln \overline{Sa}_{RD}$ and $\sigma_{\ln Sa_{RD}}$ are the logarithmic mean and standard deviation of Sa_{RD} values, respectively, that can be obtained as:

$$\ln \overline{Sa}_{RD} = \frac{1}{n} \sum_{i=1}^{n} (\ln Sa_{RD_i}) \tag{16}$$

Table 3
Damping coefficients determined for one of the FVDs added to each of stories, given different design scenarios for the structures, kN×(s/m)$^{\alpha}$.

Structure	α	Story								
		1	2	3	4	5	6	7	8	9
3-story-UD	0.25	480.24								
	0.5	892.86								
	0.75	1648.53								
	1.0	3024.46								
3-story-IDPD	0.25	422.63	524.14	480.35						
	0.5	784.29	972.68	891.46						
	0.75	1642.97	1792.58	1445.11						
	1.0	3008.68	3283.63	2647.92						
3-story-h_1-1.4-UD	0.25	948.55								
	0.5	1803.03								
	0.75	3391.50								
	1.0	6320.33								
3-story-h_1-1.4-IDPD	0.25	1258.42	730.38	587.76						
	0.5	2347.56	1362.32	1096.05						
	0.75	4335.34	2515.49	2024.69						
	1.0	7940.25	4607.59	3707.43						
9-story-UD	0.25	582.97								
	0.5	1377.11								
	0.75	3227.21								
	1.0	7509.44								
9-story-IDPD	0.25	804.26	569.26	570.94	581.97	549.21	520.22	550.21	525.81	405.80
	0.5	1887.59	1336.08	1339.71	1365.95	1288.91	1220.81	1291.42	1234.21	952.31
	0.75	4393.36	3109.75	3118.84	3178.97	2999.99	2841.28	3005.58	2872.05	2216.96
	1.0	10,152.10	7185.45	7206.47	7346.57	6933.27	6567.26	6945.53	6637.31	5122.46

$$\sigma_{\ln Sa_{RD}} = \left[\frac{1}{n-1}\sum_{i=1}^{n}\left(\ln Sa_{RD_i} - \ln\overline{Sa}_{RD}\right)^2\right]^{0.5} \quad (17)$$

where $\ln Sa_{RD_i}$ is the natural logarithm of Sa_{RD} computed using the ith record, and n is the number of ground motion records used for the analyses. It should be mentioned that the method used in this study, to obtain fragility curves, is capacity method [59], whereas the method applied by Ruiz-García and Miranda [33] is stripe method [59]. When using the capacity method, given each level of MRIDR, the logarithmic standard deviation of Sa_{RD} values, obtained by performing IDAs, is calculated. However, when using the stripe method, given each level of $Sa(T_1)$, the logarithmic standard deviation of MRIDR is calculated. In fact, the method used in this study is similar to that employed by Kitayama and Constantinou [9].

After determining the median Sa_{RD} for a structure, which is the exponential of $\ln\overline{Sa}_{RD}$, Residual Drift Margin Ratio (RDMR) can be calculated, by dividing the median Sa_{RD} of the structure by the ordinate of ASCE 7 [23] MCE_R response spectrum at the fundamental period of the structure ($Sa_{MCE_R}(T_1)$), as follows:

$$\text{RDMR} = \frac{\text{Median } Sa_{RD}}{Sa_{MCE_R}(T_1)}. \quad (18)$$

In this study, MAFs of exceeding different levels of MRIDR, i.e., λ_{RD} values, were used for evaluating the residual drift performance of the structures. To compute λ_{RD} for a specified level of MRIDR, the seismic hazard curve of the site of interest and the fragility curve corresponding to that level of MRIDR are required. Hazard curves for the site were obtained from the USGS website [60] given the periods of 0.75, 1.0, 2.0 and 3.0 s. Because the fundamental periods of the structures considered are different from these periods, the approach applied by Eads [61] was used to interpolate the hazard curves required with respect to the fundamental periods of the structures. After obtaining the hazard curve and the fragility curve

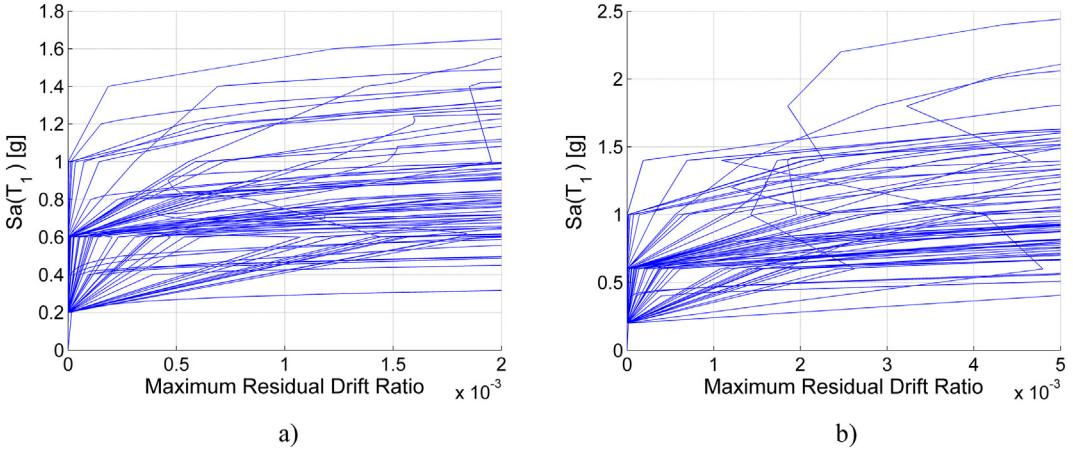

Fig. 4. IDA curves of the 3-story-UD structure with $\alpha = 0.75$ corresponding to the MRIDR levels of a) 0.2% and b) 0.5%.

corresponding to a specified level of MRIDR, λ_{RD} can be calculated as follows [9]:

$$\lambda_{RD} = \int_0^\infty P(RD|Sa) \times |d\lambda_{Sa}(Sa)| \tag{19}$$

where $P(RD|Sa)$ is the probability of exceeding the considered MRIDR value given $Sa(T_1) = Sa$, and $\lambda_{Sa}(Sa)$ is the MAF of exceeding Sa. By multiplying the right-hand side of Eq. (19) by $d(Sa)$ and dividing it by $d(Sa)$, this equation is rewritten as follows:

$$\lambda_{RD} = \int_0^\infty P(RD|Sa) \times \left|\frac{d\lambda_{Sa}(Sa)}{d(Sa)}\right| \times d(Sa) \tag{20}$$

where $\frac{d\lambda_{Sa}(Sa)}{d(Sa)}$ is the slope of the hazard curve. The integral in Eq. (20) can be calculated numerically using Eq. (21).

$$\lambda_{RD} = \sum_{i=1}^{\infty} P(RD|Sa_i) \times \left|\frac{d\lambda_{Sa}(Sa_i)}{d(Sa)}\right| \times \Delta Sa \tag{21}$$

5. Obtaining residual drift margin ratios (RDMRs) and their corresponding fragility curves

In this section, the results obtained for the SMRFs with and without FVDs are presented in the form of RDMRs and their corresponding residual drift fragilities. In addition, a comparison is conducted between the two types of vertical distributions of damping coefficients (i.e., UD and IDPD) in different levels of MRIDR. Table 4 presents the values of RDMR and their corresponding logarithmic standard deviations, $\sigma_{\ln SaRD}$, for the structures without FVDs, and the structures with FVDs given the two vertical distributions of damping coefficients. Comparing the values of RDMR for the structures with and without FVDs, indicates that adding supplemental viscous damping to the structures leads to considerable increase in the RDMR values. Furthermore, most of the values obtained for the logarithmic standard deviation of Sa_{RD}, $\sigma_{\ln SaRD}$, are in the range of 0.3–0.5. This range is in agreement with the results obtained by Kitayama and Constantinou [9].

Table 5 indicates the ratios of the median of MIDR values to the MRIDR level assumed for computing Sa_{RD} values, given the four MRIDR levels considered, for the structures with and without FVDs. To

Table 5
Ratios of the median of MIDR values to the MRIDR level assumed for computing Sa_{RD} values, given the four MRIDR levels considered, for the structures with and without FVDs.

Structure	Damper velocity α (exponent)	RD = 0.2%	RD = 0.5%	RD = 1.0%	RD = 2.0%
3-story	–	7.252	4.537	3.414	2.683
3-story-UD	0.25	6.827	3.895	2.997	2.356
	0.5	6.855	4.027	3.052	2.446
	0.75	6.983	4.105	3.119	2.461
	1.0	7.026	4.259	3.205	2.488
3-story-IDPD	0.25	6.897	4.087	3.008	2.438
	0.5	6.940	4.112	3.061	2.465
	0.75	6.997	4.138	3.156	2.481
	1.0	7.062	4.260	3.284	2.515
3-story-h_1-1.4	–	9.312	6.012	4.681	3.534
3-story-h_1-1.4-UD	0.25	8.042	4.993	3.619	2.668
	0.5	8.552	5.165	3.761	2.773
	0.75	8.773	5.225	3.940	2.938
	1.0	8.801	5.368	4.036	3.063
3-story-h_1-1.4-IDPD	0.25	8.694	5.026	3.707	2.730
	0.5	8.734	5.188	3.884	2.913
	0.75	8.756	5.409	4.043	3.118
	1.0	9.187	5.794	4.460	3.309
9-story	–	7.442	4.632	3.513	2.732
9-story-UD	0.25	6.872	4.012	2.999	2.383
	0.5	6.862	4.036	3.086	2.451
	0.75	6.987	4.156	3.136	2.460
	1.0	7.056	4.324	3.115	2.493
9-story-IDPD	0.25	6.926	4.113	3.009	2.446
	0.5	6.955	4.156	3.098	2.471
	0.75	7.013	4.183	3.199	2.496
	1.0	7.098	4.336	3.292	2.523

Table 4
Values of RDMR and $\sigma_{\ln SaRD}$ for the structures with and without FVDs.

Structure	Damper velocity α (exponent)	RDMR ($\sigma_{\ln SaRD}$)			
		RD = 0.2%	RD = 0.5%	RD = 1.0%	RD = 2.0%
3-story	–	0.302 (0.340)	0.443 (0.397)	0.724 (0.404)	1.144 (0.432)
3-story-UD	0.25	0.562 (0.309)	0.794 (0.410)	1.116 (0.472)	1.624 (0.402)
	0.5	0.594 (0.327)	0.832 (0.450)	1.192 (0.480)	1.700 (0.422)
	0.75	0.628 (0.334)	0.899 (0.477)	1.278 (0.492)	1.860 (0.441)
	1.0	0.655 (0.345)	0.997 (0.492)	1.436 (0.505)	2.034 (0.462)
3-story-IDPD	0.25	0.550 (0.281)	0.794 (0.464)	1.110 (0.475)	1.613 (0.402)
	0.5	0.567 (0.308)	0.826 (0.484)	1.173 (0.484)	1.692 (0.431)
	0.75	0.594 (0.333)	0.883 (0.489)	1.249 (0.492)	1.763 (0.441)
	1.0	0.626 (0.369)	0.967 (0.492)	1.386 (0.499)	1.961 (0.461)
3-story-h_1-1.4	–	0.420 (0.341)	0.683 (0.398)	1.021 (0.408)	1.360 (0.421)
3-story-h_1-1.4-UD	0.25	0.702 (0.345)	0.985 (0.424)	1.282 (0.396)	1.673 (0.355)
	0.5	0.777 (0.405)	1.066 (0.423)	1.386 (0.397)	1.869 (0.367)
	0.75	0.848 (0.437)	1.142 (0.430)	1.561 (0.398)	2.153 (0.383)
	1.0	0.909 (0.459)	1.215 (0.436)	1.770 (0.399)	2.524 (0.412)
3-story-h_1-1.4-IDPD	0.25	0.775 (0.382)	1.048 (0.430)	1.249 (0.391)	1.774 (0.359)
	0.5	0.845 (0.427)	1.132 (0.432)	1.497 (0.394)	1.990 (0.363)
	0.75	0.942 (0.437)	1.243 (0.435)	1.709 (0.396)	2.394 (0.390)
	1.0	0.984 (0.455)	1.347 (0.442)	1.951 (0.401)	2.619 (0.421)
9-story	–	0.376 (0.397)	0.555 (0.420)	0.879 (0.459)	1.198 (0.411)
9-story-UD	0.25	0.492 (0.306)	0.733 (0.392)	1.028 (0.434)	1.331 (0.401)
	0.5	0.540 (0.325)	0.785 (0.423)	1.122 (0.438)	1.392 (0.414)
	0.75	0.579 (0.342)	0.852 (0.447)	1.208 (0.442)	1.537 (0.428)
	1.0	0.603 (0.347)	0.935 (0.467)	1.323 (0.444)	1.717 (0.441)
9-story-IDPD	0.25	0.520 (0.319)	0.737 (0.389)	1.029 (0.434)	1.358 (0.409)
	0.5	0.540 (0.314)	0.792 (0.420)	1.154 (0.439)	1.431 (0.413)
	0.75	0.583 (0.334)	0.863 (0.445)	1.258 (0.437)	1.587 (0.435)
	1.0	0.614 (0.342)	0.941 (0.462)	1.412 (0.447)	1.839 (0.481)

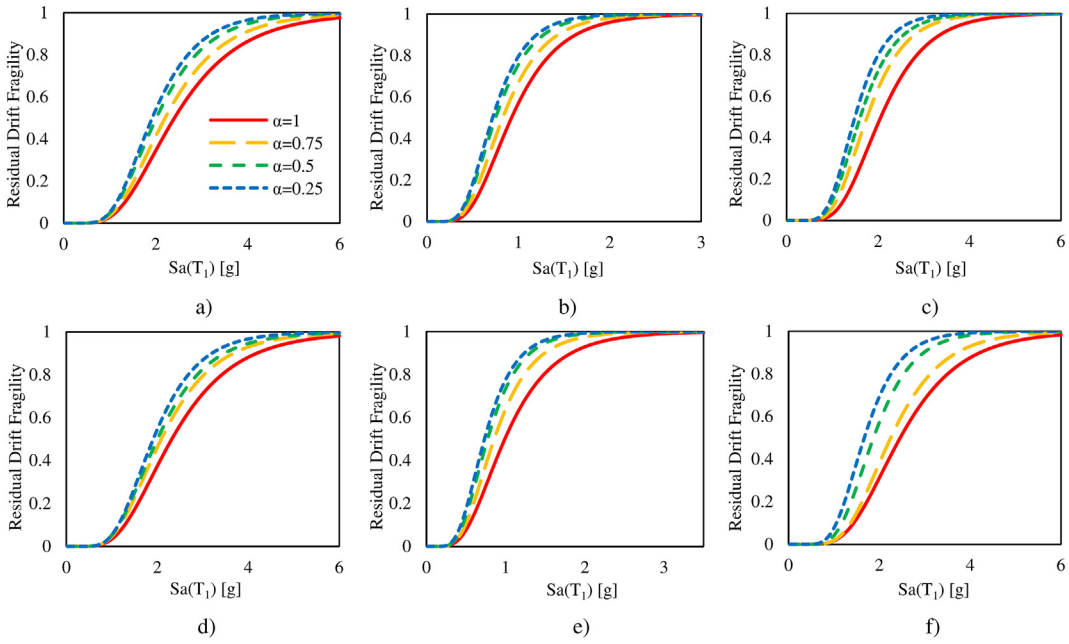

Fig. 5. Fragility curves corresponding to the limit state of MRIDR = 2.0% for a) 3-story-UD, b) 9-story-UD, c) 3-story-h_1-1.4-UD, d) 3-story-IDPD, e) 9-story-IDPD and f) 3-story-h_1-1.4-IDPD structures.

calculate these ratios for a structure, given each of the four MRIDR levels considered for obtaining Sa_{RD} values, the median of MIDR values of the structure corresponding to Sa_{RD} values was divided by the MRIDR level of interest. It can be seen that as the MRIDR level assumed increases from 0.2% to 2.0%, the ratio of the median of MIDR values to the assumed MRIDR level decreases. In fact, when a structure undergoes higher nonlinear deformations, this ratio decreases. In addition, given a level of MRIDR assumed for obtaining Sa_{RD} values, the ratio of the median of MIDR values, corresponding to Sa_{RD} values, to that MRIDR level for a structure without FVDs is higher than those for the corresponding structures with FVDs. The effects of damper velocity exponent and the vertical distribution of damping coefficients on the residual drift performance of the structures are described in the following subsections.

5.1. Investigating the effect of damper velocity exponent

According to the results presented in Table 4, it can be seen that given each of the MRIDR levels assumed, a structure equipped with linear FVDs (i.e., $\alpha = 1.0$) has a higher RDMR value than those of the corresponding structures equipped with nonlinear FVDs (i.e., $\alpha \neq 1.0$). For the structures with nonlinear FVDs, as the value of α decreases, the value of RDMR decreases correspondingly. In other words, a structure with linear FVDs has higher median Sa_{RD} values than those of the structures with nonlinear FVDs; and by decreasing the value of α, the values of median Sa_{RD} decrease. According to the results, in the worst case for the 3-story-UD structure with $\alpha = 0.25$, the value of RDMR given MRIDR = 1.0%, is 0.777 times that for the 3-story-UD structure with $\alpha = 1.0$. In the best case for this structure, the value of RDMR given MRIDR = 0.2%, is 0.858 times that for the 3-story-UD structure with $\alpha = 1.0$. In addition, in the worst case for the 3-story-h_1-1.4-UD structure with $\alpha = 0.25$, the value of RDMR given MRIDR = 2.0%, is 0.663 times that obtained assuming $\alpha = 1.0$. In the best case for the 3-story-h_1-1.4-UD structure with $\alpha = 0.25$, the value of RDMR given MRIDR = 0.5%, is 0.811 times that obtained assuming $\alpha = 1.0$. For the 9-story-UD structure with $\alpha = 0.25$, in the worst case, the value of RDMR given MRIDR = 2.0%, is 0.775 times that for the 9-story-UD structure with $\alpha = 1.0$; whereas in the best case for this structure, the value of RDMR given MRIDR = 0.2%, is 0.816 times that obtained assuming $\alpha = 1.0$. Fig. 5 illustrates the fragility curves of the structures corresponding to the limit state of MRIDR = 2.0%. It can be seen that for a specific value of $Sa(T_1)$, the probability of exceeding the desired MRIDR level for a structure equipped with linear FVDs, is lower than those for the corresponding structures equipped with nonlinear FVDs. Furthermore, among the structures with nonlinear FVDs (i.e., $\alpha =$ 0.25, 0.5 and 0.75), by increasing the value of α, the probability of exceeding the desired MRIDR level decreases. Comparing the results presented in Table 5 for similar structures with FVDs having different

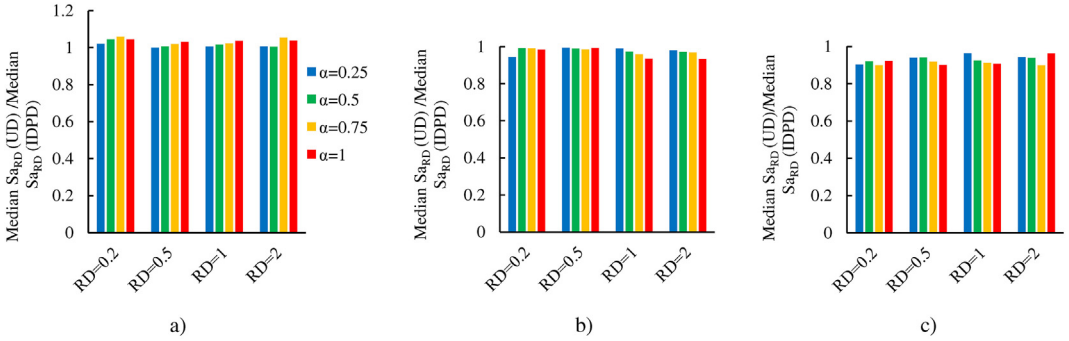

Fig. 6. Values of Median Sa_{RD} (UD)/Median Sa_{RD} (IDPD) corresponding to the different levels of MRIDR for a) 3-story, b) 9-story and c) 3-story-h_1-1.4 structures.

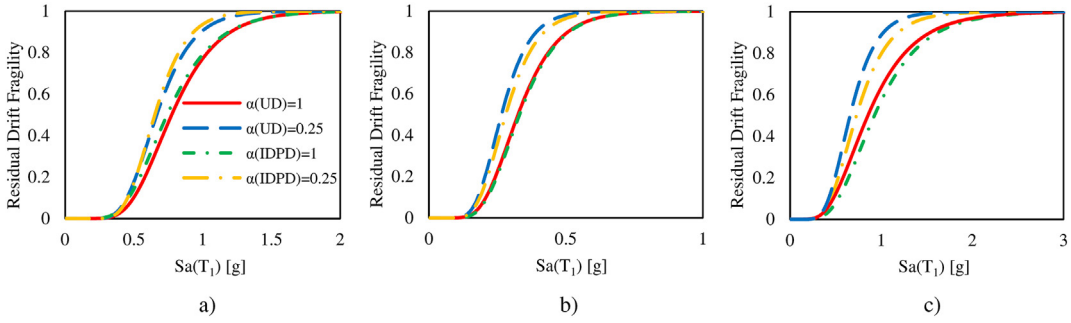

Fig. 7. Fragility curves of the structures with UD and IDPD corresponding to the limit state of MRIDR = 0.2%; a) 3-story, b) 9-story and c) 3-story-h_1-1.4.

values of α, it can be seen that given each of the MRIDR levels, decreasing α leads to decrease in the ratio of the median of MIDR values to the MRIDR level of interest.

5.2. Comparison of the vertical distributions of damping coefficients

By comparing the results presented in Table 4 for the two vertical distributions of damping coefficients, it can be seen that the values of RDMR corresponding to MRIDR = 2.0% for the 3-story-UD structures with FVDs having α values of 0.25, 0.5, 0.75 and 1.0, are 1.624, 1.70, 1.86 and 2.034, respectively; whereas the values of RDMR for the 3-story-IDPD structures are 1.613, 1.692, 1.763 and 1.961, respectively. Therefore, the values of RDMR for the 3-story-UD structure are slightly higher than those for the 3-story-IDPD structure. It should be noted the trend obtained from comparing the 9-story-UD and 9-story-IDPD structures is reverse. In other words, the RDMR values for the 9-story-IDPD structure are higher than those for the 9-story-UD structure. Furthermore, the trend obtained for the 3-story-h_1-1.4 structures is similar to that obtained for the 9-story structures. Fig. 6 compares the residual drift performance of the structures equipped with FVDs using IDPD and UD schematically. It indicates the values of median Sa_{RD} for the structures with UD normalized to the corresponding values of median Sa_{RD} for the structures with IDPD. It can be seen that the normalized values of median Sa_{RD} for the 3-story structures are higher than 1.0 (in the range of 1.001 to 1.058), whereas for the 9-story structures, the normalized values of median Sa_{RD} are lower than 1.0 (in the range of 0.934 to 0.994). Moreover, for the 3-story-h_1-1.4 structures, the normalized values of median Sa_{RD} are lower than 1.0 (in the range of 0.899 to 0.964). Therefore, it can be inferred that for the structures with a soft story, using IDPD to determine damping coefficients leads to higher RDMR values, i.e., up to 7% and 11% increase in RDMR values for the 9-story and 3-story-h_1-1.4 structures, respectively. This is because of the fact that the ductility demand of the first (soft) story is higher than those of the other stories, and when IDPD is used, the damping coefficient for the first story is greater than those for the other stories; whereas when UD is used, the damping coefficients of all the stories are identical.

Fig. 7 indicates a comparison between the fragility curves of the structures with UD and IDPD of FVDs having α values of 0.25 and 1.0. For brevity, this comparison is only for the limit state of MRIDR = 0.2%, but the same trend has been observed for the other MRIDR levels. According to this figure, the probability of exceeding the desired MRIDR level for the 3-story-UD structure with α value of 0.25 or 1.0 given a specific value of $Sa(T_1)$, is slightly lower than that for the 3-story-IDPD structure with the same value of α; whereas a reverse trend is observed for the 9-story and 3-story-h_1-1.4 structures. It can therefore be

Table 6
MAFs of exceeding different levels of MRIDR for the structures with and without FVDs.

Structure	Damper velocity α (exponent)	λ_{RD}			
		RD = 0.2%	RD = 0.5%	RD = 1.0%	RD = 2.0%
3-story	–	6.552×10^{-3}	3.184×10^{-3}	8.701×10^{-4}	2.021×10^{-4}
3-story-UD	0.25	2.371×10^{-3}	1.230×10^{-3}	5.930×10^{-4}	1.524×10^{-4}
	0.5	2.145×10^{-3}	1.199×10^{-3}	5.095×10^{-4}	1.418×10^{-4}
	0.75	1.894×10^{-3}	1.055×10^{-3}	4.365×10^{-4}	1.142×10^{-4}
	1.0	1.743×10^{-3}	8.463×10^{-4}	3.283×10^{-4}	9.307×10^{-5}
3-story-IDPD	0.25	2.403×10^{-3}	1.231×10^{-3}	6.083×10^{-4}	1.557×10^{-4}
	0.5	2.231×10^{-3}	1.229×10^{-3}	5.387×10^{-4}	1.492×10^{-4}
	0.75	2.169×10^{-3}	1.140×10^{-3}	4.657×10^{-4}	1.364×10^{-4}
	1.0	2.020×10^{-3}	9.318×10^{-4}	3.561×10^{-4}	1.046×10^{-4}
3-story-h_1_1.4	–	5.413×10^{-3}	1.938×10^{-3}	6.169×10^{-4}	2.374×10^{-4}
3-story-h_1-1.4-UD	0.25	1.482×10^{-3}	7.318×10^{-4}	3.194×10^{-4}	1.735×10^{-4}
	0.5	1.285×10^{-3}	5.898×10^{-4}	2.524×10^{-4}	8.362×10^{-5}
	0.75	1.115×10^{-3}	4.953×10^{-4}	1.746×10^{-4}	5.355×10^{-5}
	1.0	9.833×10^{-4}	4.229×10^{-4}	1.154×10^{-4}	3.428×10^{-5}
3-story-h_1-1.4-IDPD	0.25	1.237×10^{-3}	6.385×10^{-4}	2.821×10^{-4}	9.736×10^{-5}
	0.5	1.098×10^{-3}	5.125×10^{-4}	2.089×10^{-4}	6.542×10^{-5}
	0.75	8.908×10^{-4}	3.968×10^{-4}	1.282×10^{-4}	3.733×10^{-5}
	1.0	7.588×10^{-4}	3.207×10^{-4}	8.321×10^{-5}	3.126×10^{-5}
9-story	–	1.542×10^{-2}	9.167×10^{-3}	4.251×10^{-3}	2.233×10^{-3}
9-story-UD	0.25	2.312×10^{-3}	1.145×10^{-3}	5.707×10^{-4}	2.719×10^{-4}
	0.5	1.963×10^{-3}	1.037×10^{-3}	4.653×10^{-4}	2.483×10^{-4}
	0.75	1.752×10^{-3}	9.041×10^{-4}	3.914×10^{-4}	1.947×10^{-4}
	1.0	1.614×10^{-3}	7.621×10^{-4}	3.079×10^{-4}	1.466×10^{-4}
9-story-IDPD	0.25	2.101×10^{-3}	1.127×10^{-3}	5.711×10^{-4}	2.624×10^{-4}
	0.5	1.955×10^{-3}	1.005×10^{-3}	4.355×10^{-4}	2.283×10^{-4}
	0.75	1.721×10^{-3}	8.723×10^{-4}	3.643×10^{-4}	1.816×10^{-4}
	1.0	1.550×10^{-3}	7.428×10^{-4}	2.598×10^{-4}	1.373×10^{-4}

concluded that for the structures having a soft story, the probabilities of exceeding different MRIDR levels in the case of using UD, are slightly higher than the corresponding values in the case of using IDPD.

Whittle et al. [62] compared five different vertical distributions of damping coefficients and showed that using UD and SSTPD leads to similar MRIDR values. However, the results of the present study show that using UD and IDPD may lead to different residual drift performance for steel SMRFs with FVDs. The reason for difference in conclusions in terms of the effect of the vertical distribution of damping coefficients on MRIDR is that the buildings studied by Whittle et al. do not have a soft story, whereas two of the buildings considered in this study are soft-story buildings. Moreover, the study performed by Whittle et al. was limited to seismic intensities up to MCE, while the present study carries out IDA up to intensities higher than the MCE.

6. Evaluating MAFs of exceeding different levels of MRIDR

Due to the importance of MRIDR to make a decision about rebuilding or repairing of a structure after earthquake, and to estimate the insurance cost of the structure by the insurance company, the PEER PBEE framework can be applied to obtain MAFs of exceeding different levels of MRIDR (i.e., λ_{RD} values corresponding to different MRIDR levels). Table 6 indicates the values of λ_{RD} corresponding to the four previously mentioned MRIDR levels for the structures with and without FVDs. Comparing the values of λ_{RD} for the structures with and without FVDs indicates that adding supplemental viscous damping to the structures leads to considerable reductions in the values of λ_{RD}, especially for the structures with a soft story. According to the results presented in this table, it can be seen that the lowest values of λ_{RD} for all the structures with FVDs given different MRIDR levels, belong to the structures with linear FVDs. Moreover, when the value of α decreases, the value of λ_{RD} increases correspondingly. Fig. 8 illustrates the variations of λ_{RD} values of the structures with FVDs, having different values of α (i.e., α = 0.25, 0.5, 0.75 and 1.0), versus different levels of MRIDR. It can be seen that the curves in Fig. 8(a), obtained assuming different values of α, have lower dispersion compared with those in Fig. 8(b). It appears that the main difference between Fig. 8(a) and (b), which are related to the 3-story-UD and 3-story-h_1-1.4-UD structures, is due to the difference between the values of ξ_v for these structures. In other words, the values of ξ_v for these structures are 0.138 and 0.238, respectively, and increasing the value of ξ_v increases the dispersion of the curves obtained assuming different values of α. By comparing Fig. 8(d) and (e), which are related to the 3-story-IDPD and 3-story-h_1-1.4-IDPD structures, a similar trend can be observed. It is worth noting that for higher values of MRIDR the increase in dispersion between the curves is more significant.

Based on the results from the two vertical distributions of damping coefficients (i.e., UD and IDPD), presented in Table 6, the values of λ_{RD} corresponding to MRIDR = 0.2% for the 3-story-UD structures with α values of 0.25, 0.5, 0.75 and 1.0, are 2.371×10^{-3}, 2.145×10^{-3}, 1.894×10^{-3} and 1.743×10^{-3}, respectively, whereas the corresponding values of λ_{RD} for the 3-story-IDPD structures are 2.403×10^{-3}, 2.231×10^{-3}, 2.169×10^{-3} and 2.020×10^{-3}, respectively. It should be mentioned that similar trends exist for the other levels of MRIDR.

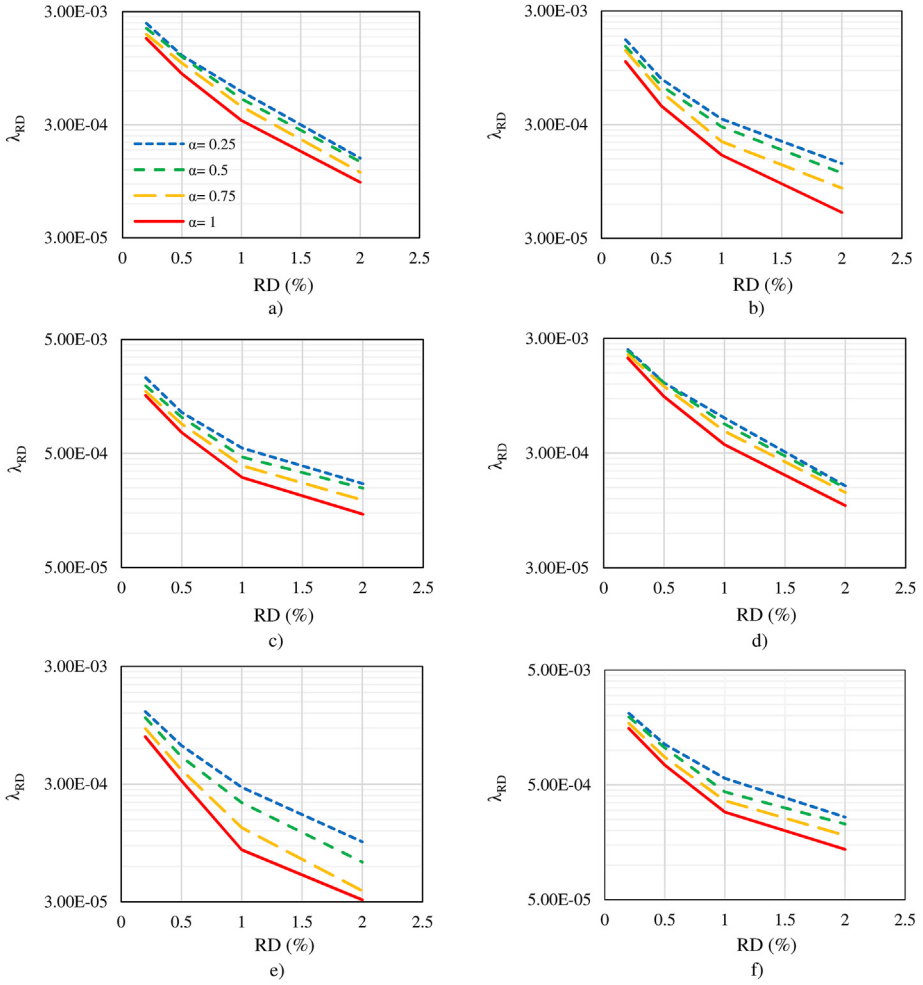

Fig. 8. Variations of λ_{RD} versus MRIDR given different values of α, for a) 3-story-UD, b) 3-story-h_1-1.4-UD, c) 9-story-UD, d) 3-story-IDPD, e) 3-story-h_1-1.4-IDPD and f) 9-story-IDPD structures.

In summary, using UD for the 3-story structure, with identical story heights, leads to an average decrease of 6.7% in λ_{RD} values calculated for the 3-story-UD structures, given all the values of α and considered MRIDR levels, compared with those for the 3-story-IDPD structures. The values of λ_{RD} corresponding to MRIDR = 0.2% for the 9-story-UD structures equipped with FVDs having α values of 0.25, 0.5, 0.75 and 1.0, are 2.312×10^{-3}, 1.963×10^{-3}, 1.752×10^{-3} and 1.614×10^{-3}, respectively, whereas the corresponding values of λ_{RD} for the 9-story-IDPD structures are 2.101×10^{-3}, 1.955×10^{-3}, 1.721×10^{-3} and 1.550×10^{-3}, respectively. A comparison of the results for the 9-story-UD and 9-story-IDPD structures given the other MRIDR levels, indicates that this trend is also valid for these MRIDR levels. In general, using IDPD for the 9-story structure, with a soft story, leads to an average decrease of 5% in λ_{RD} values calculated for the 9-story-IDPD structures, given all the values of α and considered MRIDR levels, compared with those for the 9-story-UD structures. The values of λ_{RD} corresponding to MRIDR = 0.2% for the 3-story-h_1-1.4-UD structures with α values of 0.25, 0.5, 0.75 and 1.0, are 1.482×10^{-3}, 1.285×10^{-3}, 1.115×10^{-3} and 9.833×10^{-4}, respectively, whereas the corresponding values of λ_{RD} for the 3-story-h_1-1.4-IDPD structures are 1.237×10^{-3}, 1.098×10^{-3}, 8.908×10^{-4} and 7.588×10^{-4}, respectively. Furthermore, when comparing the residual drift performance of the 3-story-h_1-1.4-UD and 3-story-h_1-1.4-IDPD structures given the other MRIDR levels, similar results are observed. In summary, in the case of the 3-story-h_1-1.4 structure, with a soft story, using IDPD leads to an average decrease of 20.8% in λ_{RD} values calculated for the 3-story-h_1-1.4-IDPD structures, given all the values of α and considered MRIDR levels, compared with those for the 3-story-h_1-1.4-UD structures. It is noteworthy that the performance improvement obtained using IDPD for this structure is more significant than that for the 9-story structure. The reason for this issue is the higher value of ξ_v for the 3-story-h_1-1.4 structure compared with that for the 9-story structure.

According to the results, given the value of ξ_v for each of the three structures considered, using Eqs. (11) to (14) for different values of α does not lead to the same value of λ_{RD}. In other words, applying these equations, existing in the technical literature, for different values of α does not guarantee the same probabilistic residual drift performance, and the value of α for FVDs certainly affects the results. It is noteworthy that Dall'Asta et al. [30] reported similar results in the case of using MIDR as an EDP. However, they considered structures equipped with FVDs that have a same mean MIDR at the design intensity level obtained from nonlinear dynamic analyses, whereas the structures considered in this study were designed to have a MIDR of 0.015 using the procedure described in Section 3, which is based on applying pushover analysis.

Fig. 9 illustrates the de-aggregation curves of residual drift hazard, given different levels of MRIDR, for the 3-story and 9-story structures with FVDs having α values of 0.25 and 1.0. Based on Eq. (21), the ordinate of each point in a de-aggregation curve is $P(RD|Sa_i) \times |\frac{d\lambda_{Sa}(Sa_i)}{d(Sa)}|$, which is the calculated by multiplying the ordinate of residual drift fragility curve, given $Sa(T_1) = Sa_i$, by the slope of seismic hazard curve given $Sa(T_1) = Sa_i$, in absolute form. It should be noted that the area under each of the curves indicates the value of λ_{RD} for the corresponding structure and MRIDR level. According to this figure, as the area under a curve increases, the regions with lower spectral accelerations have higher contribution in the area under the curve. In other words, as the desired MRIDR level decreases (i.e., MRIDR = 0.2%), lower spectral accelerations are required to reach that MRIDR level.

7. Conclusions

In this study, probabilistic residual drift assessment of steel SMRFs with linear and nonlinear FVDs was conducted. For this purpose, three SMRFs and two vertical distributions of damping coefficients including Uniform Distribution (UD) and Interstory Drift Proportional Distribution determined based on the first mode deformations (IDPD) were considered. To evaluate the effect of damper nonlinearity, four values of velocity exponent, i.e., $\alpha = 0.25$, 0.5, 0.75 and 1.0, were assumed. Moreover, four MRIDR levels were considered for performing IDAs. Then, the median MRIDR capacities (median Sa_{RD}) of the structures equipped with linear and nonlinear FVDs were estimated, and their corresponding fragility curves were developed. After developing fragility curves for different levels of MRIDR, by combining them with their

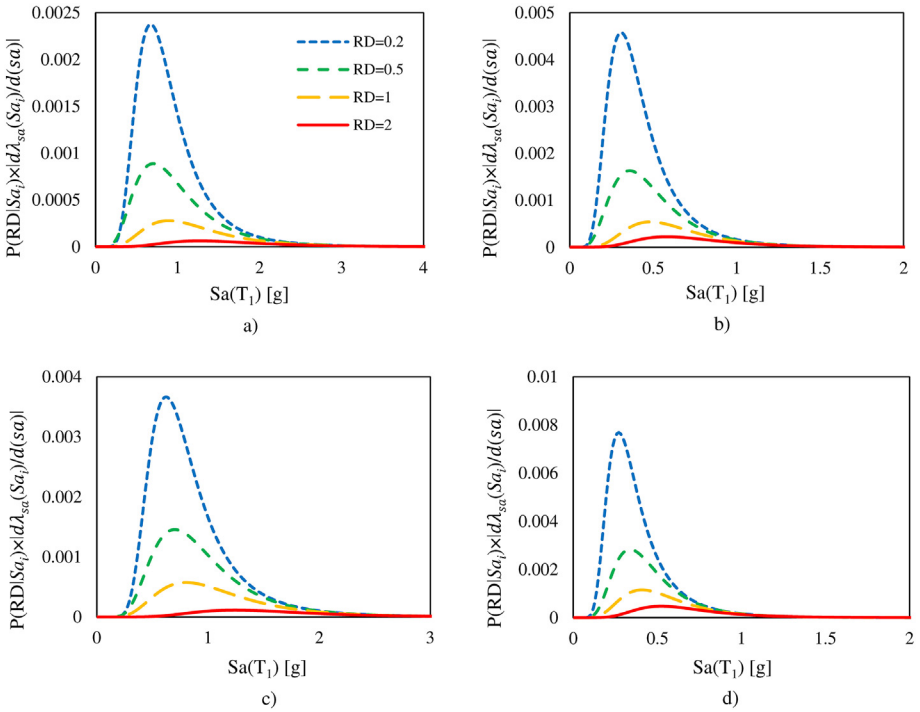

Fig. 9. De-aggregation curves of residual drift hazard given different levels of MRIDR, for a) 3-story (UD, $\alpha = 1.0$), b) 9-story (UD, $\alpha = 1.0$), c) 3-story (UD, $\alpha = 0.25$) and d) 9-story (UD, $\alpha = 0.25$) structures.

corresponding seismic hazard curve, MAFs of exceeding different levels of MRIDR (λ_{RD}) were calculated. The conclusions of this study are summarized as follows:

- The structures equipped with linear FVDs (i.e., $\alpha = 1.0$) have higher median Sa_{RD} values compared with those obtained for the corresponding structures with nonlinear FVDs (i.e., $\alpha = 0.25$, 0.5 and 0.75). Moreover, among the structures with nonlinear FVDs, as the value of α increases, the median Sa_{RD} increases correspondingly. For example, according to the results for the 3-story-h_1-1.4-UD structure, in the worst case, the Residual Drift Margin Ratio (RDMR) corresponding to $\alpha = 0.25$ and MRIDR = 2.0% is 0.663 times that corresponding to $\alpha = 1.0$.
- For each of the three structures considered, the lowest value of MAF of exceeding each MRIDR level (λ_{RD}) belongs to the structure with linear FVDs, and by decreasing the value of α, the value of λ_{RD} increases correspondingly.
- For the 3-story-h_1-1.4 structure, which has the highest value of supplemental viscous damping ratio (ξ_v) among the structures considered, the difference of λ_{RD} values given different values of α, is more obvious for higher levels of MRIDR.
- Comparing the median Sa_{RD} values obtained assuming the two vertical distributions of damping coefficients (i.e., UD and IDPD), it can be seen that using IDPD for the structures with a soft story (i.e., the 3-story-h_1-1.4 and 9-story structures) results in higher median Sa_{RD} values than those obtained using UD. However, for the 3-story structure, which does not have a soft story, using UD leads to higher median Sa_{RD} values than those obtained using IDPD.
- According to the values of λ_{RD} calculated assuming the two vertical distributions of damping coefficients (i.e., UD and IDPD), it can be concluded that using IDPD for the 3-story-h_1-1.4 and 9-story structures, with a soft story, results in average decreases of 20.8% and 5% in λ_{RD} values (given all the values of α and considered MRIDR levels), respectively, compared with those obtained using UD. Moreover, for the 3-story structure, which does not have a soft story, using UD causes an average decrease of 6.7% in λ_{RD} values, given all the values of α and considered MRIDR levels, compared with those obtained using IDPD.
- The results obtained for different MRIDR levels indicate that given the value of ξ_v for each of the three considered structures, using Eqs. (11) to (14) assuming different values of α does not result in a same λ_{RD} value, representing a same probabilistic residual drift performance. In fact, using these simplified design equations, which exist in the technical literature to proportion linear or nonlinear FVDs (with different values of α) based on a specific value of ξ_v, does not guarantee the same probabilistic residual drift performance, and the value of velocity exponent for FVDs certainly affects the results.

References

[1] J. Ruiz-García, E. Miranda, Evaluation of residual drift demands in regular multi-storey frames for performance-based seismic assessment, Earthq. Eng. Struct. Dyn. 35 (13) (2006) 1609–1629, https://doi.org/10.1002/eqe.593.

[2] E. Bojórquez, J. Ruiz-García, Residual drift demands in moment-resisting steel frames subjected to narrow-band earthquake ground motions, Earthq. Eng. Struct. Dyn. 42 (11) (2013) 1583–1598, https://doi.org/10.1002/eqe.2288.

[3] C. Christopoulos, S. Pampanin, M.J.N. Priestley, Performance-based seismic response of frame structures including residual deformations part I: single-degree of freedom systems, J. Earthq. Eng. 7 (1) (2003) 97–118, https://doi.org/10.1142/S1363246903000894.

[4] J. Ruiz-García, J.D. Aguilar, Aftershock seismic assessment taking into account postmainshock residual drifts, Earthq. Eng. Struct. Dyn. 44 (9) (2015) 1391–1407, https://doi.org/10.1002/eqe.2523.

[5] P. Sultana, M.A. Youssef, Seismic performance of steel moment resisting frames utilizing superelastic shape memory alloys, J. Constr. Steel Res. 125 (2016) 239–251, https://doi.org/10.1016/j.jcsr.2016.06.019.

[6] J. McCormick, H. Aburano, M. Ikenaga, M. Nakashima, Permissible residual deformation levels for building structures considering both safety and human elements, Proceedings of the 14th World Conference on Earthquake Engineering, Beijing, China, 2008.

[7] FEMA P-58-1, Seismic Performance Assessment of Buildings Volume 1—Methodology, Federal Emergency Management Agency, Washington, DC, 2012.

[8] B.S.S. Council, FEMA 356, Prestandard and Commentary for the Seismic Rehabilitation of Buildings, Federal Emergency Management Agency, Washington, DC, 2000.

[9] S. Kitayama, M.C. Constantinou, Probabilistic collapse resistance and residual drift assessment of buildings with fluidic self-centering systems, Earthq. Eng. Struct. Dyn. 45 (12) (2016) 1935–1953, https://doi.org/10.1002/eqe.2733.

[10] T.T. Soong, B.F. Spencer, Supplemental energy dissipation: state-of-the-art and state-of-the-practice, Eng. Struct. 24 (3) (2002) 243–259, https://doi.org/10.1016/S0141-0296(01)00092-X.

[11] A.A. Seleemah, M.C. Constantinou, Investigation of Seismic Response of Buildings with Linear and Nonlinear Fluid Viscous Dampers, National Center for Earthquake Engineering Research, Buffalo, NY, 1997.

[12] C. Christopoulos, A. Filiatrault, Principles of Passive Supplemental Damping and Seismic Isolation, IUSS Press, Pavia, 2006.

[13] Taylor Devices Inc., http://taylordevices.com/dampers-seismic-protection.html 2018, Accessed date: 20 January 2018.

[14] Jarret Structures, http://www.jarretstructures.com/en/doc/BROCH_vd.pdf 2018, Accessed date: 20 January 2018.

[15] M.C. Constantinou, M.D. Symans, Experimental and Analytical Investigation of Seismic Response of Structures with Supplemental Fluid Viscous Dampers, National Center for Earthquake Engineering Research, Buffalo, NY, 1992.

[16] M.R. Mansoori, A.S. Moghadam, Using viscous damper distribution to reduce multiple seismic responses of asymmetric structures, J. Constr. Steel Res. 65 (12) (2009) 2176–2185, https://doi.org/10.1016/j.jcsr.2009.06.016.

[17] J. Kim, J. Lee, H. Kang, Seismic retrofit of special truss moment frames using viscous dampers, J. Constr. Steel Res. 123 (2016) 53–67, https://doi.org/10.1016/j.jcsr.2016.04.027.

[18] H.R. Jamshidiha, M. Yakhchalian, B. Mohebi, Advanced scalar intensity measures for collapse capacity prediction of steel moment resisting frames with fluid viscous dampers, Soil Dyn. Earthq. Eng. 109 (2018) 102–118, https://doi.org/10.1016/j.soildyn.2018.01.009.

[19] T.L. Karavasilis, C.Y. Seo, Seismic structural and non-structural performance evaluation of highly damped self-centering and conventional systems, Eng. Struct. 33 (8) (2011) 2248–2258, https://doi.org/10.1016/j.engstruct.2011.04.001.

[20] A. Bahnasy, O. Lavan, Linear or nonlinear fluid viscous dampers? A seismic point of view, Structures Congress: Bridging Your Passion with Your Profession 2013, pp. 2253–2264.

[21] A.S. Whittaker, M.C. Constantinou, O.M. Ramirez, M.W. Johnson, C.Z. Chrysostomou, Equivalent lateral force and modal analysis procedures of the 2000 NEHRP provisions for buildings with damping systems, Earthquake Spectra 19 (4) (2003) 959–980, https://doi.org/10.1193/1.1622391.

[22] B.S.S. Council, FEMA 368, NEHRP Recommended Provisions for Seismic Regulations for New Buildings and Other Structures Part 1: Provisions, National Institute of Building Sciences, Washington, DC, 2000.

[23] ASCE/SEI 7-10, Minimum Design Loads for Buildings and Other Structures, American Society of Civil Engineers, Reston, VA, 2010.

[24] L. Landi, S. Lucchi, P.P. Diotallevi, A procedure for the direct determination of the required supplemental damping for the seismic retrofit with viscous dampers, Eng. Struct. 71 (2014) 137–149, https://doi.org/10.1016/j.engstruct.2014.04.025.

[25] L. Landi, F. Conti, P.P. Diotallevi, Effectiveness of different distributions of viscous damping coefficients for the seismic retrofit of regular and irregular RC frames, Eng. Struct. 100 (2015) 79–93, https://doi.org/10.1016/j.engstruct.2015.05.031.

[26] C.A. Cornell, H. Krawinkler, Progress and Challenges in Seismic Performance Assessment, PEER Center News, 2000, 3.

[27] H. Krawinkler, A general approach to seismic performance assessment, Proceedings of International Conference on Advances and New Challenges in Earthquake Engineering Research, Vol. 3, Harbin and Hong Kong, China, Hong Kong, 2002, pp. 173–180.

[28] K.A. Porter, An overview of PEER's performance-based earthquake engineering methodology, Proceedings of Ninth International Conference on Applications of Statistics and Probability in Civil Engineering, 2003.

[29] J. Moehle, G.G. Deierlein, A framework methodology for performance-based earthquake engineering, Proceedings of the 13th World Conference on Earthquake Engineering, Vancouver, Canada, 2004, pp. 3812–3814.

[30] A. Dall'Asta, E. Tubaldi, L. Ragni, Influence of the nonlinear behavior of viscous dampers on the seismic demand hazard of building frames, Earthq. Eng. Struct. Dyn. 45 (1) (2016) 149–169, https://doi.org/10.1002/eqe.2623.

[31] E. Tubaldi, L. Ragni, A. Dall'Asta, Probabilistic seismic response assessment of linear systems equipped with nonlinear viscous dampers, Earthq. Eng. Struct. Dyn. 44 (1) (2015) 101–120, https://doi.org/10.1002/eqe.2461.

[32] A. Dall'Asta, F. Scozzese, L. Ragni, E. Tubaldi, Effect of the damper property variability on the seismic reliability of linear systems equipped with viscous dampers, Bull. Earthq. Eng. 15 (11) (2017) 5025–5053, https://doi.org/10.1007/s10518-017-0169-8.

[33] J. Ruiz-García, E. Miranda, Probabilistic estimation of residual drift demands for seismic assessment of multi-story framed buildings, Eng. Struct. 32 (1) (2010) 11–20, https://doi.org/10.1016/j.engstruct.2009.08.010.

[34] A. Deylami, M.A. Mahdavipour, Probabilistic seismic demand assessment of residual drift for buckling-restrained braced frames as a dual system, Struct. Saf. 58 (2016) 31–39, https://doi.org/10.1016/j.strusafe.2015.08.004.

[35] A.I. Dimopoulos, A.S. Tzimas, T.L. Karavasilis, D. Vamvatsikos, Probabilistic economic seismic loss estimation in steel buildings using post-tensioned moment-resisting frames and viscous dampers, Earthq. Eng. Struct. Dyn. 45 (11) (2016) 1725–1741, https://doi.org/10.1002/eqe.2722.

[36] A.S. Tzimas, G.S. Kamaris, T.L. Karavasilis, C. Galasso, Collapse risk and residual drift performance of steel buildings using post-tensioned MRFs and viscous dampers in

near-fault regions, Bull. Earthq. Eng. 14 (6) (2016) 1643–1662, https://doi.org/10.1007/s10518-016-9898-3.
[37] D. Vamvatsikos, C.A. Cornell, Incremental dynamic analysis, Earthq. Eng. Struct. Dyn. 31 (3) (2002) 491–514, https://doi.org/10.1002/eqe.141.
[38] Uniform Building Code, Structural engineering design provisions, Vol. 2, International Conference of Building Officials, Whittier, CA, 1994.
[39] SAC Joint Venture, Proceedings of the Invitational Workshop on Steel Seismic Issues, Report No. SAC 94-01, Los Angeles, CA, 1994.
[40] H. Krawinkler, FEMA-355C, State of the Art Report on Systems Performance of Steel Moment Frames Subject to Earthquake Ground Shaking. Prepared for the SAC Joint Venture, Published by the Federal Emergency Management Agency, Washington, DC, 2000.
[41] G. Apostolakis, G.F. Dargush, Optimal seismic design of moment-resisting steel frames with hysteretic passive devices, Earthq. Eng. Struct. Dyn. 39 (4) (2010) 355–376, https://doi.org/10.1002/eqe.944.
[42] M. Hamidia, A. Filiatrault, A. Aref, Simplified Seismic Collapse Capacity-Based Evaluation and Design of Frame Buildings with and without Supplemental Damping Systems. Report No. MCEER-14-0001, Multidisciplinary Center for Earthquake Engineering Research, Buffalo, NY, 2014.
[43] C.B. Haselton, G.G. Deierlein, Assessing Seismic Collapse Safety of Modern Reinforced Concrete Moment-Frame Buildings, Report No. PEER 2007/08, Pacific Earthquake Engineering Research Center, Berkeley, CA, 2008.
[44] U.S. Geological Survey, https://earthquake.usgs.gov/designmaps/us/application.php 2016, Accessed date: 30 November 2016.
[45] O.M. Ramirez, M.C. Constantinou, C.A. Kircher, A.S. Whittaker, M.W. Johnson, J.D. Gomez, C.Z. Chrysostomou, Development and Evaluation of Simplified Procedures for Analysis and Design of Buildings with Passive Energy Dissipation Systems, Report No. MCEER-00-0010 Revision 1, Multidisciplinary Center for Earthquake Engineering Research, Buffalo, NY, 2001.
[46] F. McKenna, G.L. Fenves, M.H. Scott, Open System for Earthquake Engineering Simulation, Pacific Earthquake Engineering Research Center, Berkeley, CA, 2015.
[47] C.Y. Seo, T.L. Karavasilis, J.M. Ricles, R. Sause, Seismic performance and probabilistic collapse resistance assessment of steel moment resisting frames with fluid viscous dampers, Earthq. Eng. Struct. Dyn. 43 (14) (2014) 2135–2154, https://doi.org/10.1002/eqe.2440.
[48] L.F. Ibarra, H. Krawinkler, Global Collapse of Frame Structures under Seismic Excitations, Report No. PEER 2005/06, Pacific Earthquake Engineering Research Center, Berkeley, CA, 2005.
[49] D.G. Lignos, H. Krawinkler, Deterioration modeling of steel components in support of collapse prediction of steel moment frames under earthquake loading, J. Struct. Eng. 137 (11) (2010) 1291–1302, https://doi.org/10.1061/(ASCE)ST.1943-541X.0000376.
[50] Min LL PP. Norme Tecniche per le Costruzioni. Italian Building Code, Adopted with D.M. 14/01/2008, published on S.O. n. 30 G.U, 2008.
[51] N. Luco, B.R. Ellingwood, R.O. Hamburger, J.D. Hooper, J.K. Kimball, C.A. Kircher, Risk-targeted versus current seismic design maps for the conterminous United States, Proceedings of SEAOC 2007 Convention, Structural Engineers Association of California, Sacramento, CA, 2007.
[52] J.M. Londoño, D.J. Wagg, S.A. Neild, Supporting brace sizing in structures with added linear viscous fluid dampers: a filter design solution, Earthq. Eng. Struct. Dyn. 43 (13) (2014) 1999–2013, https://doi.org/10.1002/eqe.2433.
[53] W.H. Lin, A.K. Chopra, Earthquake response of elastic single-degree-of-freedom systems with nonlinear viscoelastic dampers, J. Eng. Mech. 129 (6) (2003) 597–606, https://doi.org/10.1061/(ASCE)0733-9399(2003)129:6(597).
[54] T.L. Karavasilis, Assessment of capacity design of columns in steel moment resisting frames with viscous dampers, Soil Dyn. Earthq. Eng. 88 (2016) 215–222, https://doi.org/10.1016/j.soildyn.2016.06.006.
[55] K. Kariniotakis, T.L. Karavasilis, Modified capacity design rule for columns in tall steel MRFs with linear viscous dampers within the framework of Eurocode 8, Bull. Earthq. Eng. 16 (2) (2018) 917–932, https://doi.org/10.1007/s10518-017-0230-7.
[56] M. Yakhchalian, G. Ghodrati Amiri, A. Nicknam, A new proxy for ground motion selection in seismic collapse assessment of tall buildings, Struct. Des. Tall Spec. Build. 23 (17) (2014) 1275–1293, https://doi.org/10.1002/tal.1143.
[57] M. Yakhchalian, A. Nicknam, G. Ghodrati Amiri, Optimal vector-valued intensity measure for seismic collapse assessment of structures, Earthq. Eng. Eng. Vib. 14 (1) (2015) 37–54, https://doi.org/10.1007/s11803-015-0005-6.
[58] M. Yakhchalian, G. Ghodrati Amiri, M. Eghbali, (2017). Reliable seismic collapse assessment of short-period structures using new proxies for ground motion record selection. Sci. Iran. 24 (5) (2017) 2283–2293, https://doi.org/10.24200/SCI.2017.4162.
[59] J.W. Baker, Vector-Valued Ground Motion Intensity Measures for Probabilistic Seismic Demand Analysis, PhD Dissertation, Department of Civil and Environmental Engineering, Stanford University, Stanford, CA, 2005.
[60] U.S. Geological Survey, http://geohazards.usgs.gov/hazardtool/application.php 2016, Accessed date: 30 December 2016.
[61] L. Eads, Seismic Collapse Risk Assessment of Buildings: Effects of Intensity Measure Selection and Computational Approach, PhD Dissertation, Stanford University, Stanford, CA, 2013.
[62] J.K. Whittle, M.S. Williams, T.L. Karavasilis, A. Blakeborough, A comparison of viscous damper placement methods for improving seismic building design, J. Earthq. Eng. 16 (4) (2012) 540–560, https://doi.org/10.1080/13632469.2011.653864.